

The Polarized Single-Crystal Visible Spectrum of $\text{Mo}_2(\text{O}_2\text{CCPh}_3)_4$

F. Albert Cotton* and Bianxiao Zhong

Contribution from the Department of Chemistry and Laboratory for Molecular Structure and Bonding, Texas A&M University, College Station, Texas 77843. Received June 21, 1989

Abstract: The title compound crystallizes from CH_2Cl_2 as large yellow tetragonal crystals ($P4/ncc$) in which all Mo–Mo bonds are parallel to the crystal c axis and intermolecular interactions are only of the weak van der Waals type. The ideal formula of the substance is $\text{Mo}_2(\text{O}_2\text{CCPh}_3)_4 \cdot 3\text{CH}_2\text{Cl}_2$, but real crystals are incompletely solvated to varying degrees depending on thermal history. From polarized spectra at 6 K of such single crystals having different degrees of partial solvation, as well as from the study of several hot bands, it has been shown that the electronic absorption band with its origin at about 450 nm should be assigned to the ${}^1\text{A}_{1g} \rightarrow {}^1\text{A}_{2u}$ ($\delta \rightarrow \delta^*$) electronic transition. In axial polarization the principal progression-building vibration is the Mo–Mo stretch in the ${}^1\text{A}_{2u}$ state (ca. 370 cm^{-1}), and hot-band studies give a ground-state frequency of ca. 410 cm^{-1} , in good agreement with Raman spectra of other $\text{Mo}_2(\text{O}_2\text{CR})_4$ compounds. In the perpendicularly polarized spectra, there are progressions built on origins 239, 267, 495, and 546 cm^{-1} above the axial origin, and these can be attributed to vibronic transitions based on E_g vibrational modes.

The problem of correctly assigning, and fully interpreting the vibronic structure of, a weak absorption band that occurs around 23 000 cm^{-1} in all $\text{Mo}_2(\text{O}_2\text{CR})_4$ compounds has a long and somewhat tortuous history.¹ Although the assignment of this band to the $\delta \rightarrow \delta^*$ excitation (or ${}^1\text{A}_{1g} \rightarrow {}^1\text{A}_{2u}$ transition) was supported by $X\alpha$ -SW calculations,^{2,3} acceptance of this assignment was delayed by experimental problems. In D_{4h} , this spin-allowed transition is dipole allowed in z polarization. However, comparable intensities in both z and xy polarizations were observed in polarized spectral studies on $\text{Mo}_2(\text{O}_2\text{CCH}_2\text{NH}_3)_4(\text{SO}_4)_2 \cdot 4\text{H}_2\text{O}^4$ and $\text{Mo}_2(\text{O}_2\text{CH})_4$.⁵ From this, it was concluded that the band could not be assigned to a $\delta \rightarrow \delta^*$ transition. Instead, it was believed that both the z and xy structures were due to vibronic intensities from some other, dipole-forbidden, transition. A year later, detailed studies on $\text{Mo}_2(\text{O}_2\text{CCH}_3)_4$ and $\text{Mo}_2(\text{O}_2\text{CCF}_3)_4$ were reported.⁶ Here, intensities in xy polarization were found to be predominant, and the electronic origin was assigned to the dipole-forbidden $\delta \rightarrow \pi^*$, ${}^1\text{A}_{1g} \rightarrow {}^1\text{E}_g$ transition, which could have gained intensity from vibronic coupling. The spectra of $\text{Mo}_2(\text{O}_2\text{CCH}_3)_4$ were reexamined by Martin, Newman, and Fanwick in 1979.⁷ They assigned the peak in z polarization with the lowest energy to the $\delta \rightarrow \delta^*$ transition and suggested that the same transition developed intensity in xy polarization via vibronic coupling. They proposed that the intensity of the dipole-allowed $\delta \rightarrow \delta^*$ transition was so low that the intensities of vibronically excited lines in xy polarization approached the intensity of the dipole-allowed progression. A study of dimolybdenum–amino acid complexes supported this conclusion.⁸

A significant problem in the studies of $\text{Mo}_2(\text{O}_2\text{CCH}_3)_4$ crystals by Martin et al.⁷ and Trogler et al.⁶ is that there is a triclinic lattice and the molecules reside on sites with $\bar{1}$ symmetry. The possibility that some electronically forbidden transitions can gain intensity by lowering of the symmetry (from D_{4h}) cannot be excluded for molecules in an environment of such low symmetry. Even more serious is the fact that, in principle, there are no rigorously defined

molecular optical axes for molecules that are in nonuniaxial crystals. Indeed, in the acetate, the transition moment is 34° away from the z axis and it was conjectured by Martin et al.⁷ that the molecular z polarization was shifted from the molecular z axis by the crystal field perturbations. Finally, in these compounds the geometric arrangement is such that the molecules are not aligned in any simple relationship either to the lattice vectors or among themselves. In the crystals of the amino acid complexes, molecular alignment was, fortuitously, convenient for the spectroscopist, but the other problems were still present.

If a crystal is the tetragonal system, such as a $\text{Mo}_2(\text{O}_2\text{CCPh}_3)_4 \cdot 3\text{CH}_2\text{Cl}_2$ crystal, and if the $\delta \rightarrow \delta^*$ assignment is correct, the transition moment should be exactly parallel to the molecular z axis. Moreover, a tetragonal crystal is uniaxial, and the molecular site symmetry is nearly as high as the idealized molecular symmetry per se. One final reason why we were interested in the crystal spectra of $\text{Mo}_2(\text{O}_2\text{CCPh}_3)_4 \cdot 3\text{CH}_2\text{Cl}_2$ is because it is unlike all other $\text{Mo}_2(\text{O}_2\text{CR})_4$ compounds, in which there are intermolecular bonds between the Mo atoms and the oxygen atoms of adjacent dimers.¹ No such bonds exist in $\text{Mo}_2(\text{O}_2\text{CCPh}_3)_4$ because the carboxyl oxygen atoms in $\text{Mo}_2(\text{O}_2\text{CCPh}_3)_4$ molecules are prevented by the phenyl rings from using their lone pairs to reach the Mo atoms of neighbors, and the solvent CH_2Cl_2 is a noncoordinating molecule. Therefore, we may see whether axial coordination has much effect on the energy of the electronic transitions.

The crystal structure of $\text{Mo}_2(\text{O}_2\text{CCPh}_3)_4 \cdot 3\text{CH}_2\text{Cl}_2$ has been reported in detail elsewhere.⁹ For our purposes here, we need only recall that the $\text{Mo}_2(\text{O}_2\text{CCPh}_3)_4$ molecules are rigorously aligned with the crystal c axis in a unit cell in space group $P4/ncc$, and that there are sites for CH_2Cl_2 molecules of two types. One type places these CH_2Cl_2 molecules in pockets close to the ends of the Mo–Mo axes, where they can engage in weak axial interactions with the Mo_2 units. The other sites are separated from the Mo_2 chromophore by a considerable distance (ca. 10 Å) because of the bulk of the CPh_3 groups. We would expect that the CH_2Cl_2 molecules on sites of the first type are more difficult to expel, and only these molecules may be expected to have significant effects on the vibrational wave functions of the Mo–Mo stretching modes, and hence on the Franck–Condon factors.

Experimental Section

The crystal spectra were recorded on a Cary 17-D spectrophotometer using equipment and methods that have been described in earlier papers from this laboratory.¹⁰

(9) Cotton, F. A.; Kibala, P. A.; Shamshoum, E. S.; Zhong, B. Manuscript in preparation.

(1) Cotton, F. A.; Walton, R. A. *Multiple Bonds Between Metal Atoms*; John Wiley & Sons: New York, 1982.

(2) Mortola, A. P.; Moskowitz, J. W.; Rosch, N.; Cowman, C. D.; Gray, H. B. *Chem. Phys. Lett.* **1975**, *32*, 283.

(3) Norman, J. G.; Kolari, H. J. *J. Am. Chem. Soc.* **1975**, *97*, 33.

(4) Cotton, F. A.; Martin, D. S.; Webb, T. R.; Peters, T. J. *Inorg. Chem.* **1976**, *15*, 1199.

(5) Cotton, F. A.; Martin, D. S.; Fanwick, P. E.; Peters, T. J.; Webb, T. R. *J. Am. Chem. Soc.* **1976**, *98*, 4681.

(6) Trogler, W. C.; Solomon, E. I.; Trabjerg, I.; Ballhausen, C. J.; Gray, H. B. *Inorg. Chem.* **1977**, *16*, 628.

(7) Martin, D. S.; Newman, R. A.; Fanwick, P. E. *Inorg. Chem.* **1979**, *18*, 2511.

(8) Bino, A.; Cotton, F. A.; Fanwick, P. E. *Inorg. Chem.* **1980**, *19*, 1215.

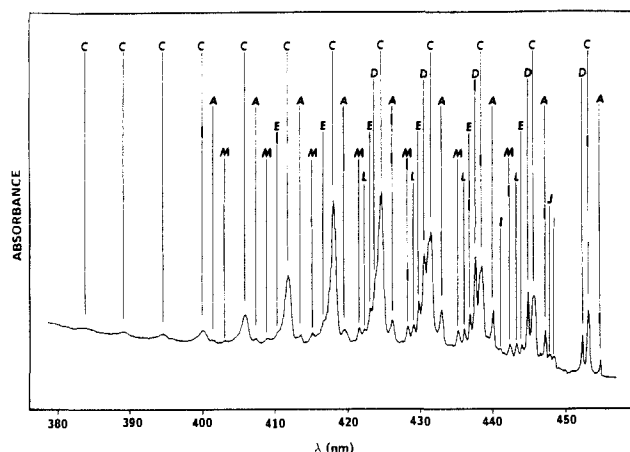


Figure 1. Single-crystal-polarized spectrum of $\text{Mo}_2(\text{O}_2\text{CPh}_3)_4 \cdot (\text{CH}_2\text{Cl}_2)_3$ at 6 K. Polarization is parallel to the molecular z or the crystallographic c axis. The crystal is in the space group $P4/ncc$. At this polarization angle, A, C, D, and E progressions reach their maxima and the other progressions reach their minima. Spectral bandwidth is less than 0.15 nm.

Table I. Vibrational Structures in the z -Polarized Absorption Spectrum of $\text{Mo}_2(\text{O}_2\text{CPh}_3)_4 \cdot 3\text{CH}_2\text{Cl}_2^a$

line	$\bar{\nu}$, cm^{-1}	$\Delta\bar{\nu}$, cm^{-1}	line	$\bar{\nu}$, cm^{-1}	$\Delta\bar{\nu}$, cm^{-1}
A ₀	21 993		C ₆	24 284	363
A ₁	22 364	371	C ₇	24 643	359
A ₂	22 732	368	C ₈	25 003	360
A ₃	23 105	372	C ₉	25 361	358
A ₄	23 474	371	C ₁₀	25 717	356
A ₅	23 840	366	D ₀	22 113	(120)
A ₆	24 187	347	D ₁	22 485	372
A ₇	24 552	365	D ₂	22 856	371
A ₈	24 917	365	D ₃	23 229	373
C ₀	22 073	(80)	D ₄	23 602	373
C ₁	22 443	370	E ₀	22 528	(535)
C ₂	22 812	369	E ₁	22 901	373
C ₃	23 180	368	E ₂	23 274	373
C ₄	23 553	373	E ₃	23 639	365
C ₅	23 921	368	E ₄	24 009	370

^a Values in parentheses are the $\Delta\bar{\nu}$ from the A₀ line. Values without parentheses are $\Delta\bar{\nu}$ from the preceding line in the progression.

The crystals of $\text{Mo}_2(\text{O}_2\text{CPh}_3)_4 \cdot 3\text{CH}_2\text{Cl}_2$ were prepared as described elsewhere,⁹ but with some modifications favoring the growth of crystals with habits and size more suited to the present work. After the reaction mixture in CH_2Cl_2 had been refluxed and filtered, it was concentrated to one-fourth its volume. This caused a yellow powder to separate, but all of this redissolved on warming. This clear solution was then slowly cooled, and large yellow crystals appeared. Examination of these on the X-ray diffractometer showed that they had the same unit cell as the smaller ones previously used in the structure determination. It was found that the crystal c axis is parallel to the longest edge in all examined crystals.

Results and Discussion

The spectra at 6 K in the molecular z and xy polarizations for crystals of $\text{Mo}_2(\text{O}_2\text{CPh}_3)_4 \cdot 3\text{CH}_2\text{Cl}_2$ are shown in Figures 1 and 2. The spectra are well resolved and have very rich vibrational structures. The results, although much more complicated than those of $\text{Mo}_2(\text{O}_2\text{CCH}_3)_4$, support the assignment by Martin et al.⁷

Tables I and II record the wave numbers of all observed lines and shoulders. All vibrational progressions have about the same spacing, 370 cm^{-1} . There are four z -polarized progressions, of which A, C, and D are rather intense and E is much weaker. All other progressions are xy -polarized. When the spectra were recorded at different polarized angles, it was found that the intensities of the A, C, D, and E progressions attained maxima when

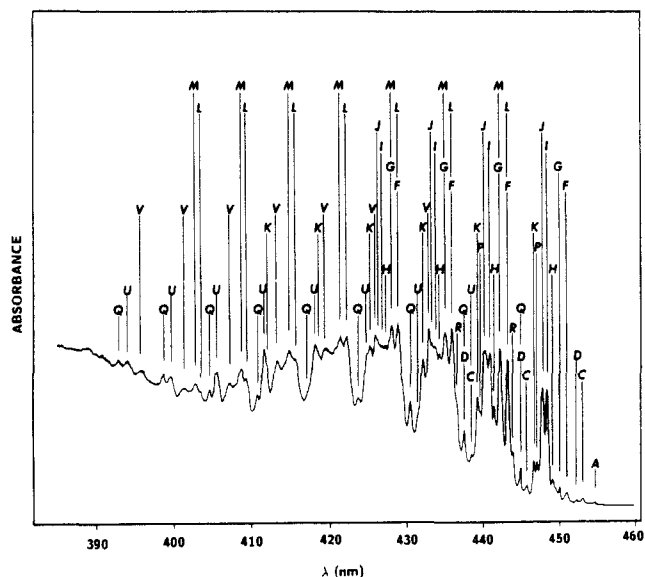


Figure 2. Single-crystal-polarized spectrum of $\text{Mo}_2(\text{O}_2\text{CPh}_3)_4 \cdot (\text{CH}_2\text{Cl}_2)_3$ at 6 K. Polarization is perpendicular to the molecular z or the crystallographic c axis. The crystal is in the space group $P4/ncc$. At this polarization angle, A, C, D, and E progressions reach their minima and the other progressions reach their maxima. Spectral bandwidth is less than 0.15 nm.

Table II. Vibrational Structures in the xy -Polarized Absorption Spectrum of $\text{Mo}_2(\text{O}_2\text{CPh}_3)_4 \cdot 3\text{CH}_2\text{Cl}_2^a$

line	$\bar{\nu}$, cm^{-1}	$\Delta\bar{\nu}$, cm^{-1}	line	$\bar{\nu}$, cm^{-1}	$\Delta\bar{\nu}$, cm^{-1}
F ₀	22 183	(190)	L ₂	23 313	376
G ₀	22 231	(238)	L ₃	23 683	370
H ₀	22 277	(284)	L ₄	24 050	367
H ₁	22 659	382	L ₅	24 422	372
H ₂	23 030	371	L ₆	24 783	361
I ₀	22 312	(317)	M ₀	22 619	(626)
I ₁	22 686	374	M ₁	22 990	371
I ₂	23 059	373	M ₂	23 356	366
J ₀	22 340	(347)	M ₃	23 732	376
J ₁	22 711	371	M ₄	24 103	371
J ₂	23 085	374	M ₅	24 467	364
P ₀	22 381	(388)	M ₆	24 823	356
P ₁	22 747	366	V ₀	23 103	(1110)
K ₀	22 403	(410)	V ₁	23 478	375
K ₁	22 770	367	V ₂	23 843	365
K ₂	23 145	375	V ₃	24 194	351
K ₃	23 512	367	V ₄	24 552	358
Q ₀	22 491	(498)	V ₅	24 916	364
Q ₁	22 862	371	V ₆	25 261	345
Q ₂	23 232	370	U ₀	22 813	(820)
Q ₃	23 604	372	U ₁	sh	
Q ₄	sh		U ₂	23 542	
Q ₅	24 342		U ₃	23 906	364
Q ₆	24 712	370	U ₄	24 291	385
Q ₇	25 077	365	U ₅	24 657	366
Q ₈	25 450	373	U ₆	25 022	365
L ₀	22 568	(575)	U ₇	25 374	352
L ₁	22 937	369	R ₀	22 540	(547)

^a Values in parentheses are the $\Delta\bar{\nu}$ from the A₀ line. Values without parentheses are $\Delta\bar{\nu}$ from the preceding line in the progression.

the polarization plane was parallel to the crystal c axis or molecular z axis, and minima when the polarization plane was 90° to the axis. The lowest energy features occur in the z polarization, and thus the electronic origin should be a z -dipole-allowed transition. This is consistent with the $\delta \rightarrow \delta^*$ assignment of the transition.

It is surprising that there are so many vibrational progressions in both the z and xy polarizations. For $\text{Mo}_2(\text{O}_2\text{CCH}_3)_4$, only two z -polarized progressions were seen.⁷ One of them was assigned to the $\delta \rightarrow \delta^*$ transition combined with the totally symmetric Mo–Mo stretching vibration. The other progression, which was 320 cm^{-1} above the first one, was thought to be due to the addition of an A_{1g} vibration of 320 cm^{-1} to the 0–0 energy.⁷ For Mo_2 -

(10) (a) Cotton, F. A.; Fanwick, P. E. *J. Am. Chem. Soc.* **1979**, *101*, 5252. (b) Cotton, F. A.; Fanwick, P. E.; Gage, L. D. *J. Am. Chem. Soc.* **1980**, *102*, 1570.

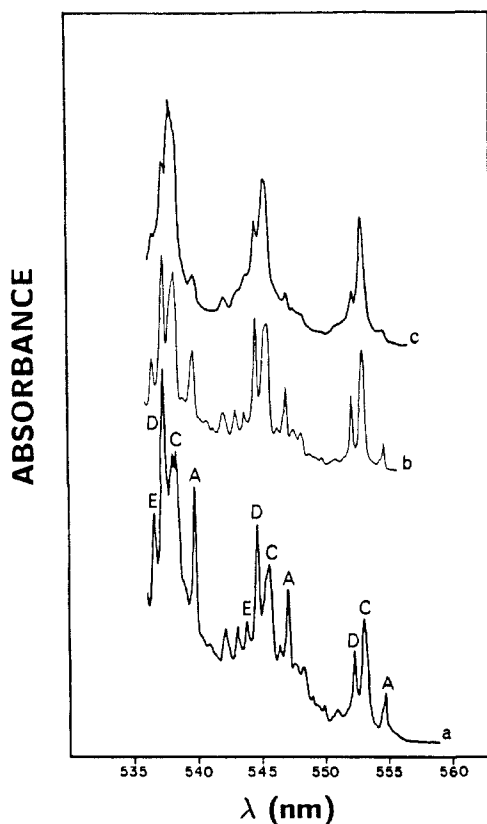


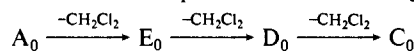
Figure 3. Effects of the solvent on the vibrational structures in the *z*-polarized spectra of $\text{Mo}_2(\text{O}_2\text{CCPh}_3)_4$: (a) the crystal subjected to an Ar stream for 30 min; (b) the crystal subjected to an Ar stream for 70 min; (c) the crystal placed under Ar for 70 min and then under vacuum for 20 min.

$(\text{O}_2\text{CCPh}_3)_4 \cdot 3\text{CH}_2\text{Cl}_2$ we cannot assign the C and D progressions in the same way because C_0 or D_0 is only 80 or 120 cm^{-1} above A_0 , and no A_{1g} vibrations have such low frequencies. The C and D progressions are too intense to be phonon bands of A progressions. A possible explanation is that some of the progressions might be due to impurities such as $\text{Mo}_2(\text{O}_2\text{CCPh}_3)_3(\text{O}_2\text{CCH}_3)$. It was reported that the 18% impurity of $\text{Mo}_2(\text{mhp})_3(\text{O}_2\text{CCH}_3)$ in $\text{Mo}_2(\text{mhp})_4$ caused several vibrational components.¹¹ To check this possibility, $\text{Mo}_2(\text{O}_2\text{CCPh}_3)_4 \cdot 3\text{CH}_2\text{Cl}_2$ was prepared from $\text{K}_4\text{Mo}_2\text{Cl}_8$ instead of $\text{Mo}_2(\text{O}_2\text{CCH}_3)_4$. In a typical preparation, 0.10 g of $\text{K}_4\text{Mo}_2\text{Cl}_8$ was reacted with 0.24 g of HO_2CCPh_3 in 10 mL of MeOH at reflux temperature for 1 h, resulting in a yellow precipitate. The precipitate was then washed with MeOH, dried by heating under vacuum, and then recrystallized from CH_2Cl_2 , resulting in large yellow crystals. The spectra of these crystals are the same as those of the crystals made from $\text{Mo}_2(\text{O}_2\text{CCH}_3)_4$, and therefore, the rich vibrational structures cannot be attributed to incompletely substituted impurities.

Another hypothesis, probably the only other one, is that the CH_2Cl_2 molecules in the crystal, which are easily lost by evaporation, may be responsible. According to the crystal structural results,⁹ there are four $\text{Mo}_2(\text{O}_2\text{CCPh}_3)_4$ dimers and 12 CH_2Cl_2 molecules in each unit cell. Eight of the CH_2Cl_2 molecules are near the axial positions. The distance between the Mo atoms and Cl atoms in those solvent molecules is about 3.8 Å. The other four CH_2Cl_2 molecules are on 4-fold axes, and they are far away from the Mo atoms (about 10 Å). The loss of some of these solvent molecules means that some $\text{Mo}_2(\text{O}_2\text{CCPh}_3)_4$ dimers may lose one adjacent CH_2Cl_2 molecule, and some may lose two or more CH_2Cl_2 molecules. The energy of the $\delta \rightarrow \delta^*$ transition may then be slightly different, depending on the local environment of solvent molecules. Therefore, several progressions, one for each type of

environment, could appear. The relative intensities of those progressions should depend on the extent of loss of solvent molecules.

To verify the above hypothesis, the spectra of several crystals, which either had been subjected to an Ar stream for different periods of time or had been placed under vacuum at room temperature, were measured. As shown in Figure 3, the ratio $I(\text{A}_0):I(\text{C}_0):I(\text{D}_0):I(\text{E}_0)$ does depend on the extent of solvent loss. For a, b, and c, the values for the ratio $I(\text{A}_0):I(\text{C}_0):I(\text{D}_0):I(\text{E}_0)$ are 16:46:25:13, 11:50:28:11, and 4:70:18:8, respectively. When the crystals were exposed to an Ar stream at room temperature for increasing lengths of time (from a to b), the intensity of A_0 decreased rapidly, that of E_0 decreased more slowly, and those of C_0 and D_0 increased. It seems likely that the A progression is due to the dimers that have lost no adjacent CH_2Cl_2 molecules and that the E, C, and D progressions all represent the dimers that have lost some solvent molecules. After a crystal had been pumped for 20 min (from b to c), the intensities of A_0 and E_0 decreased, that of D_0 decreased substantially, and that of C_0 gained. Thus, the C progression may correspond to those dimers that have lost the most neighboring solvent molecules, and the D progression may represent those that have easily lost some solvent and can then lose more solvent under more rigorous conditions. We can thus express this solvent-losing process as



Let us look now at the intensity distribution pattern in each progression in Figure 1. In the A progression, the third line (A_2) is the highest and the fourth and the second have similar heights. For D or E, the third is the highest but the fourth is lower than the second. The C progression has a totally different pattern: the fifth line is highest, and the sixth is higher than the fourth. The patterns for the A, D, and E progressions are similar to each other, and they are also similar to that obtained for $\text{Mo}_2(\text{O}_2\text{CCH}_3)_4$.⁷ Since intensity patterns are dependent on Frank–Condon factors, the C vibrational structure has a Frank–Condon factor different from the others. This may be because the dimers represented by C have lost a CH_2Cl_2 molecule at the axial position and the solvent molecule at this position may have effects on the vibrational wave functions of the Mo–Mo stretching mode and, therefore, have some effect on the magnitude of the overlap integral $\int \Psi_{\nu'}^*(R) \Psi_{\nu}(R) d\tau_{\nu}$, whose square is the Frank–Condon factor. This is consistent with the fact that the C progression is assigned to those dimers that lost more solvent under more rigorous conditions and that the solvent molecules at axial positions should be more difficult to expel than those far away from Mo atoms due to the weak interaction between the axial Cl in CH_2Cl_2 and the Mo atoms.

If we attribute the four vibrational progressions in *z* polarization to the $\delta \rightarrow \delta^*$ electronic origin combined with the totally symmetric Mo–Mo stretching mode of molecules in four kinds of environments caused by solvent loss, we can understand why there are so many progressions in *xy* polarization. The $\delta \rightarrow \delta^*$ transition has A_{2u} symmetry, so that the addition of E_g vibrational modes to the origin will result in *xy*-allowed transitions. $\text{Mo}_2(\text{O}_2\text{CCH}_3)_4$ has two such vibrational modes coupled to the $\delta \rightarrow \delta^*$ transition, the 275 and the 545- cm^{-1} vibrations, that are two of the five E_g degenerate pairs of vibrations of the Mo–O–C framework.⁷ The intense vibronic lines in the spectrum of $\text{Mo}_2(\text{O}_2\text{CCPh}_3)_4 \cdot 3\text{CH}_2\text{Cl}_2$ (Figure 2) can also be attributed to these two vibrations. As shown in Figure 2 and Table II, I_0 and J_0 are, respectively, 239 and 267 cm^{-1} above C_0 and thus they may be due to the addition of either a 239- or 267- cm^{-1} vibration to the C_0 origin. These two vibrations correspond to the degenerate 275- cm^{-1} E_g vibration in the case of $\text{Mo}_2(\text{O}_2\text{CCH}_3)_4$. We would expect much greater site-symmetry perturbation for CPh_3 groups than for the CH_3 group, and thus we may expect the splitting of the degenerate E_g pair for $\text{Mo}_2(\text{O}_2\text{CCPh}_3)_4 \cdot 3\text{CH}_2\text{Cl}_2$. Similarly, L_0 and M_0 could be due to the addition of the 495- and 546- cm^{-1} vibrational pair to the C_0 origin, and this pair corresponds to the 545- cm^{-1} pair in $\text{Mo}_2(\text{O}_2\text{CCH}_3)_4$. Similarly, the additions of the same two pairs of vibrational modes to the origin A_0 result in H_0 and G_0 , and Q_0 and R_0 . For the origin D_0 , only K_0 and P_0 resulting from the 275- cm^{-1} pair can be seen;

(11) Fanwick, P. E.; Bursten, B. E.; Kaufmann, G. B. *Inorg. Chem.* **1985**, *24*, 1165.

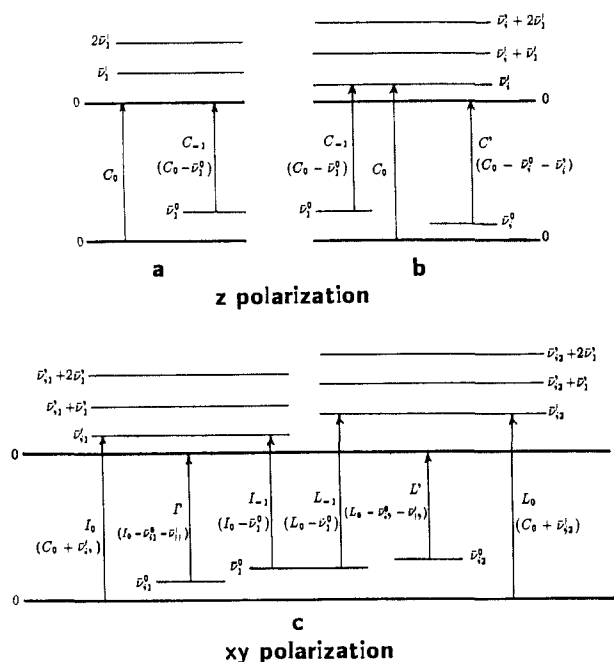


Figure 4. Possible hot bands for the z polarization (a or b) and the xy polarization (c): (a) an electric dipole allowed electronic transition with an A_{1g} vibration; (b) an imagined situation in which the z -polarized C_0 were a vibronic origin (a dipole-forbidden transition plus a nontotally symmetric vibration), where $\bar{\nu}_i^1$ or $\bar{\nu}_i^0$ is the wavenumber for the vibration in the excited or ground state; (c) two vibronic origins, L_0 and I_0 , in the xy polarization.

the other two lines resulting from the 545-cm^{-1} pair are probably superimposed by H_1 and I_1 . U_0 and V_0 are, respectively, 285 and 485 cm^{-1} above E_0 , so they could be the vibronic lines for E_0 . All features except the weak F_0 line in Figure 2 can be assigned, if the totally symmetric Mo-Mo stretching mode is added to each of the vibronic origins resulting from the two pairs of vibrational modes. F_0 might be due to the addition of a new vibrational mode to the origin C_0 , but more likely, it could be derived from a different electronic state. A similar band was also reported for $\text{Mo}_2(\text{O}_2\text{CCF}_3)_4$.¹²

An excellent experiment to verify our assignments is to examine hot bands by using a thick crystal. The most important questions are the following: Is our assignment of A_0 , C_0 , D_0 , and E_0 to the electric dipole allowed $\delta \rightarrow \delta^*$ transition correct? Should they be assigned to electric dipole forbidden vibronic transitions? If our assignment of the dipole-allowed electronic origin is correct, are the xy -polarized lines derived from this origin?

As indicated in Figure 4a, if C_0 is a dipole-allowed electronic origin, it should have one hot band C_{-1} at lower energy. On the other hand, if C_0 is a dipole-forbidden vibronic origin with $\bar{\nu}_i^1$ the wavenumber for a nontotally symmetric vibration, we would expect a second hot band C' with an energy ($\bar{\nu}_i^0 + \bar{\nu}_i^1$) lower than C_0 (Figure 4b). The hot bands of a $\text{Mo}_2(\text{O}_2\text{CPh}_3)_4 \cdot 3\text{CH}_2\text{Cl}_2$ crystal with a thickness of 1 mm in z polarization at various temperatures are shown in Figure 5. Indeed, only a single hot band was observed, which confirms our assignment of the electric dipole allowed origin. Actually, the hot band has contributions from A_0 , C_0 , and D_0 , which are so close to each other that they appear as a single and broad peak for a thick crystal at high temperatures. With the help of Figure 4a, we can get the ground-state vibrational frequency $\bar{\nu}_1^0$ of the Mo-Mo totally symmetric mode by taking the energy difference between the hot band and the combined peaks of A_0 , C_0 , and D_0 . This frequency turns out to be 410 cm^{-1} , 40 cm^{-1} higher than the excited-state frequency (370 cm^{-1}) exhibited in all vibrational progressions. This is in good agreement with the reported Raman frequency of 404 cm^{-1} for $\nu(\text{Mo-Mo})$ in $\text{Mo}_2(\text{O}_2\text{CCH}_3)_4$ at 20 K ¹³ and with that of $\text{Mo}_2(\text{O}_2\text{CCH}_3)_4$ (400

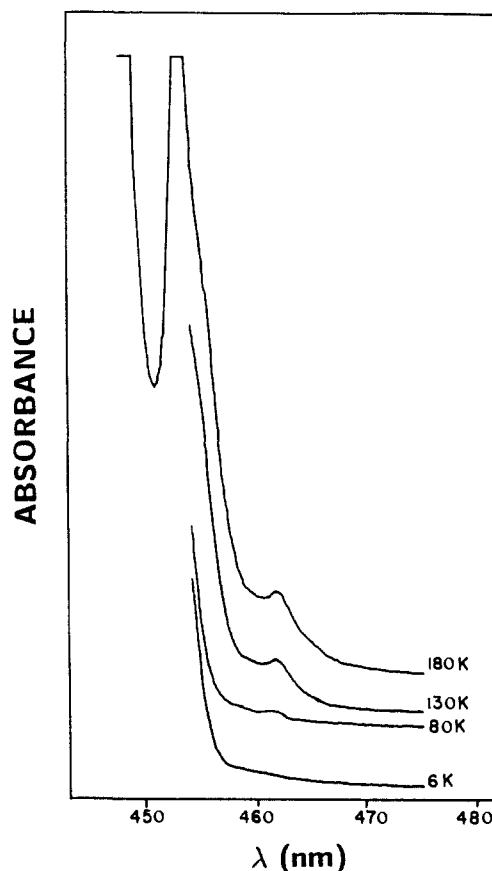


Figure 5. Hot bands in the z -polarized spectrum of a $\text{Mo}_2(\text{O}_2\text{CPh}_3)_4 \cdot 3\text{CH}_2\text{Cl}_2$ crystal with a thickness of 1 mm. The only observed hot band is at $21\,645\text{ cm}^{-1}$, 410 cm^{-1} below the combined peak ($22\,326\text{ cm}^{-1}$) of A_0 , C_0 , and D_0 .

cm^{-1})⁷ within the experimental uncertainty for $\bar{\nu}_1^0$.

We can also calculate the probability that for C_0 there is a second hot band that is too weak to observe. Let us assume that the second band, C' , can be seen only if its intensity is one-tenth that of C_{-1} or higher. Then we have the following equations:

$$I(C')/I(C_{-1}) \approx \frac{e^{-\bar{\nu}_i^0/kT}}{e^{-\bar{\nu}_i^1/kT}} = e^{(\bar{\nu}_i^1 - \bar{\nu}_i^0)/kT} \geq 0.1$$

$$\bar{\nu}_i^0 \leq \bar{\nu}_i^1 - kT \ln 0.1 = 698\text{ cm}^{-1} (180\text{ K})$$

Therefore, we may not observe a second existing hot band if $\bar{\nu}_i^0$ is larger than 700 cm^{-1} .

We can also verify the assignment for the dipole-allowed origin in z polarization by examining vibronic hot bands in xy polarization. If the hot-band study can prove those vibronic origins are derived from A_0 , C_0 , and D_0 , then those origins must be *dipole-allowed in z polarization* (but forbidden in xy polarization).

As indicated in Figure 4c, there should be four hot bands, I_{-1} , I' , L_{-1} , and L' , each of which has contributions from the combined peaks of $I_0 + J_0$ or $L_0 + M_0$. But L_{-1} will not be observed because it happens to be at the same position as F_0 if our assignments for the vibronic origins in xy polarization are correct. The experimental results are presented in Figure 6. Indeed, all three expected hot bands based on our assignments (Figure 4c) appeared at higher temperatures. The energy difference between the $21\,913\text{ cm}^{-1}$ and the combined peak of I_0 and J_0 ($22\,326\text{ cm}^{-1}$) is 413 cm^{-1} , corresponding to the ground-state frequency ν_1^0 of the totally symmetric mode. So the $21\,913\text{-cm}^{-1}$ line is L_{-1} in Figure 4c. Similarly, the $21\,777\text{-cm}^{-1}$ line is 549 cm^{-1} below the combined peak of I_0 and J_0 , so this hot band should be I' and the value 549 cm^{-1} corresponds to $(\nu_1^0 + \nu'_{11})$. The average ν'_{11} calculated from $(I_0 - C_0)$ and $(J_0 - C_0)$ is 253 cm^{-1} , so ν_{11}^0 , the ground-state frequency

(12) Manning, M. C.; Holland, G. F.; Ellis, D. E.; Trogler, W. C. *J. Phys. Chem.* **1983**, *87*, 3083.

(13) Clark, R. J. H.; Hempleman, A. J.; Kurmoo, M. *J. Chem. Soc., Dalton Trans.* **1988**, 973.

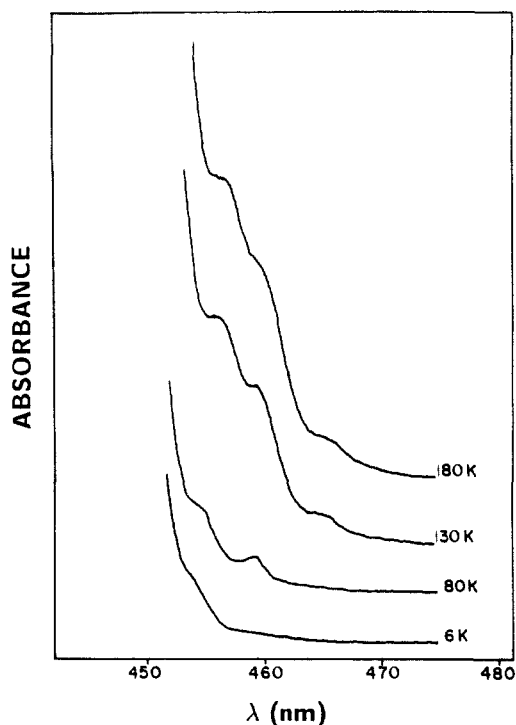


Figure 6. Hot bands in the *xy*-polarized spectrum of a $\text{Mo}_2(\text{O}_2\text{CCPh}_3)_4 \cdot 3\text{CH}_2\text{Cl}_2$ crystal with a thickness of 1 mm. The three observed bands are at 21 913, 21 777, and 21 475 cm^{-1} .

of one of the E_g vibration pairs, is 296 cm^{-1} , almost the same as the reported value 295 cm^{-1} for $\text{Mo}_2(\text{O}_2\text{CCH}_3)_4$.⁷ Actually, a fairly intense Raman band at 301 cm^{-1} was reported for $\nu(\text{Mo}-\text{O})$ in $\text{Mo}_2(\text{O}_2\text{CCH}_3)_4$.¹³ The third hot band (21 475 cm^{-1}) is 1119 cm^{-1} below the peak ($L_0 + M_0$) at 22 594 cm^{-1} , and this band is L' . A value of 598 cm^{-1} can be obtained from this band for ν_{12}^0 . The appearance of L' is a little surprising because no corresponding band was observed for $\text{Mo}_2(\text{O}_2\text{CCH}_3)_4$.⁷ The reason may be that the crystal we used is much thicker than the one used for the $\text{Mo}_2(\text{O}_2\text{CCH}_3)_4$ study, and therefore, we can observe weak hot bands. This can be seen more clearly by performing the following calculations. The intensity ratio $I(L')/I(L_{-1})$ at 180 K can be calculated as follows:

$$\begin{aligned} I(L')/I(L_{-1}) &= [e^{-598/kT}I(L_0)]/[e^{-410/kT}I(I_0)] \\ &= e^{-188/kT} \times I(L_0)/I(I_0) \\ &= 0.22[I(L_0)/I(I_0)] \end{aligned}$$

From Figure 2, we know I_0 and L_0 are of about the same intensity, so $I(L')$ is about 22% of $I(L_{-1})$. This result means we should be able to see L' at 180 K as we actually did. In Figure

6, the observed ratio of $I(L')$ to $I(L_{-1})$ is near the calculated one. At 80 K, the calculated ratio is 0.03, and L_{-1} is pretty weak itself, so L' is not observable as shown in Figure 6. A similar calculation can explain why I' is more intense than L_{-1} . We should mention that the weak vibronic origins, F_0 , G_0 , H_0 , P_0 , K_0 , Q_0 , and R_0 , should also give rise to hot bands, but they are too weak to observe under our experimental conditions.

The hot-band study in *xy* polarization on $\text{Mo}_2(\text{O}_2\text{CCPh}_3)_4 \cdot 3\text{CH}_2\text{Cl}_2$ has verified the conclusion that the lines in *xy* polarization are derived from the dipole-forbidden origins, which are the same origins in the *z* polarization, by addition of two E_g vibrational modes. The results also provide strong evidence to support the assignment of the *z*-polarized origins to the dipole-allowed $\delta \rightarrow \delta^*$ transition.

The spectra of $\text{Mo}_2(\text{O}_2\text{CCPh}_3)_4 \cdot 3\text{CH}_2\text{Cl}_2$ have provided valuable support for the conclusion of Martin et al.,⁷ not only because their conclusion can well explain such complicated spectra but also because the detailed hot-band study verified the assignments. The particular importance of this work is that the well-resolved *z*-polarization or *xy*-polarization structures are directly observed in the direction parallel or perpendicular to the molecular *z* axis in a tetragonal crystal that has excluded the uncertainty caused by the large deviation of the transition moment from the molecular *z* axis in crystals with lower lattice symmetry as $\text{Mo}_2(\text{O}_2\text{CCH}_3)_4$ ⁷ or $\text{Mo}_2(\text{O}_2\text{CH})_4$.⁵ In the case of the formate, the deviation was so large that the observed polarization was reversed.⁵

Another special feature of $\text{Mo}_2(\text{O}_2\text{CCPh}_3)_4 \cdot 3\text{CH}_2\text{Cl}_2$ is that it has no axial coordination. It is interesting to see how different the energy of the dipole-allowed transition in this compound is from that of the other compounds. Actually, there is no significant difference as indicated by the following values: $\text{Mo}_2(\text{O}_2\text{CCPh}_3)_4 \cdot 3\text{CH}_2\text{Cl}_2$, 22 073 cm^{-1} ; $\text{Mo}_2(\text{O}_2\text{CCF}_3)_4$, 22 070 cm^{-1} .⁷ $\text{Mo}_2(\text{O}_2\text{CH})_4$, 21 870 cm^{-1} .⁵ $\text{Mo}_2(\text{O}_2\text{CCH}_3)_4$, 21 700 cm^{-1} .⁷ This is consistent with the assignment of the $\delta \rightarrow \delta^*$ transition because the orbital from an axial molecule is orthogonal to both δ and δ^* orbitals and, thus, the energies of δ and δ^* orbitals will not change when the axial ligand is not present, and the Mo-Mo distance should be essentially unchanged (which is also true).

Conclusions

Despite the complexity of the spectra we have obtained for $\text{Mo}_2(\text{O}_2\text{CCPh}_3)_4 \cdot x\text{CH}_2\text{Cl}_2$ crystals, because of their varying degrees of solvation, the polarized spectra, together with the results for hot bands, provide the strongest evidence yet (in our opinion, conclusive evidence) for assigning the weak feature that occurs in the spectra of all $\text{Mo}_2(\text{O}_2\text{CR})_4$ compounds to the ${}^1A_{1g} \rightarrow {}^1A_{2u}$ ($\delta \rightarrow \delta^*$) transition.

Acknowledgment. We thank the National Science Foundation for support and Dr. L. R. Falvello for guidance and assistance in the operation of the spectroscopic equipment.

Registry No. $\text{Mo}_2(\text{O}_2\text{CCPh}_3)_4$, 124561-76-8; $\text{Mo}_2(\text{O}_2\text{CCPh}_3)_4 \cdot 3\text{CH}_2\text{Cl}_2$, 124561-77-9.